Biogeosciences, 11, 5155–5168, 2014
www.biogeosciences.net/11/5155/2014/
doi:10.5194/bg-11-5155-2014

Biogeosciences Open Access

Modern and Cenozoic records of seawater magnesium from foraminiferal Mg isotopes

P. A. E. Pogge von Strandmann[1,2], J. Forshaw[1,*], and D. N. Schmidt[1]

[1]Bristol Isotope Group, School of Earth Sciences, Bristol, UK
[2]Institute of Earth and Planetary Sciences, University College London and Birkbeck University of London, Gower Street, London, WC1E 6BT, UK
[*]now at: Department of Earth Sciences, Kingston University London, London, UK

Correspondence to: P. A. E. Pogge von Strandmann (p.strandmann@ucl.ac.uk)

Received: 1 May 2014 – Published in Biogeosciences Discuss.: 23 May 2014
Revised: 8 August 2014 – Accepted: 28 August 2014 – Published: 25 September 2014

Abstract. Magnesium is an element critically involved in the carbon cycle, because weathering of Ca-Mg silicates removes atmospheric CO_2 into rivers, and formation of Ca-Mg carbonates in the oceans removes carbon from the ocean-atmosphere system. Hence the Mg cycle holds the potential to provide valuable insights into Cenozoic climate-system history, and the shift during this time from a greenhouse to icehouse state. We present Mg isotope ratios for the past 40 Myr using planktic foraminifers as an archive. Modern foraminifera, which discriminate against elemental and isotopically heavy Mg during calcification, show no correlation between the Mg isotope composition (δ^{26}Mg, relative to DSM-3) and temperature, Mg / Ca or other parameters such as carbonate saturation (ΔCO_3). However, inter-species isotopic differences imply that only well-calibrated single species should be used for reconstruction of past seawater. Seawater δ^{26}Mg inferred from the foraminiferal record decreased from ~ 0 ‰ at 15 Ma, to -0.83 ‰ at the present day, which coincides with increases in seawater lithium and oxygen isotope ratios. It strongly suggests that neither Mg concentrations nor isotope ratios are at steady state in modern oceans, given its ~ 10 Myr residence time. From these data, we have developed a dynamic box model to understand and constrain changes in Mg sources to the oceans (rivers) and Mg sinks (dolomitisation and hydrothermal alteration). Our estimates of seawater Mg concentrations through time are similar to those independently determined by pore waters and fluid inclusions. Modelling suggests that dolomite formation and the riverine Mg flux are the primary controls on the δ^{26}Mg of seawater, while hydrothermal Mg removal and the δ^{26}Mg of rivers are more minor controls. Using Mg riverine flux and isotope ratios inferred from the $^{87}Sr/^{86}Sr$ record, the modelled Mg removal by dolomite formation shows minima in the Oligocene and at the present day (with decreasing trends from 15 Ma), both coinciding with rapid decreases in global temperatures.

1 Introduction

The weathering of Ca-Mg silicates sequesters atmospheric CO_2 and controls long-term climate (Walker et al., 1981; Berner et al., 1983; Kump et al., 2000). In turn, the history of weathering on land is partly reflected by the Mg evolution of the ocean, recorded by marine carbonates. Given that Mg is critically involved in the long-term carbon cycle, studying Mg isotopes offers advantages over trace elements that are not involved so directly, such as strontium or osmium isotopes (Palmer and Edmond, 1992; Levasseur et al., 1999; Georg et al., 2013). The dominant Mg source to the oceans is thought to be continental weathering, via rivers and groundwater, while the main sinks are removal by hydrothermal fluids (primarily by high-temperature interaction with basalt, which is thought to quantitatively strip Mg from fluids), dolomite formation and low-temperature clay formation during alteration of the oceanic crust (Holland, 2005).

Reconstructing the sources and sinks of past seawater Mg contents through time, however, demands deconvolving Mg uptake by these carbonate archives as well as variations in Mg sources and sinks to seawater (Holland, 2005).

Importantly, the fundamental question whether Mg in the oceans is in steady state is still unanswered (Holland, 2005; Tipper et al., 2006b), although most recent studies suggest that seawater Mg concentrations are rapidly evolving with time (Coggon et al., 2010; Higgins and Schrag, 2012; Horita et al., 2002; Fantle and DePaolo, 2006).

The various seawater sources and sinks have different Mg isotope ratios, providing the basis for using Mg isotopes to understand long-term Mg cycling. The flux-weighted mean riverine input has a δ^{26}Mg (‰ deviation of the sample $^{26}Mg/^{24}Mg$ ratio from the standard DSM-3) of -1.09 ± 0.05 ‰ that is intermediate between that of silicate and carbonate sources. Additional fractionation is caused by Mg uptake into plants, or into secondary minerals formed during weathering (Tipper et al., 2010, 2006a, b, 2008; Pogge von Strandmann et al., 2008, 2011, 2012; Teng et al., 2010a, b; Huang et al., 2012; Black et al., 2006; Bolou-Bi et al., 2012, 2007). Modern oceans, which are isotopically uniform (Foster et al., 2010; Young and Galy, 2004), have an isotope ratio (-0.83 ± 0.01 ‰) close to the riverine input. Quantitative removal of Mg from the oceans (i.e. causing no isotope fractionation) (Holland, 2005; Tipper et al., 2006b) by high-temperature hydrothermal processes is considered to be the main sink, with hydrothermal circulation a potential, to date unconstrained, secondary factor (Mottl and Wheat, 1994). Dolomite (and to a far lesser extent calcite) formation imparts isotope fractionation (by 1.7–2 ‰), driving residual seawater isotopically heavy (Geske et al., 2012; Higgins and Schrag, 2010a).

Magnesium isotopes in marine carbonates have potential for deconvolving these parameters. A mechanistic understanding of the uptake of Mg into calcite would also significantly enhance our ability to use foraminifers as an archive. Foraminifers have strong control over the Mg uptake into their carbonate, discriminating against Mg during biomineralisation, with test Mg / Ca $\sim$ 1000–3000 times lower than seawater Mg / Ca (Lea et al., 1999). Despite this strong biomineralisation control, due to temperature-dependent uptake during calcification, Mg in foraminifers is a proxy for palaeotemperatures (Anand et al., 2003; Elderfield and Ganssen, 2000; Nürnberg et al., 1996; Martinez-Boti et al., 2011; Lear et al., 2000). Foraminifera discriminate against heavy Mg isotopes, with foraminiferal carbonate being over 5 ‰ lighter than seawater, and $\sim$ 2.5 ‰ lighter than inorganic carbonate (Chang et al., 2004; Pogge von Strandmann, 2008; Wombacher et al., 2011; Li et al., 2012; Saulnier et al., 2012; Yoshimura et al., 2011; Saenger and Wang, 2014). There is significant species-specific fractionation (Pogge von Strandmann, 2008; Wombacher et al., 2011; Chang et al., 2004), although the causes of this fractionation are not yet understood.

While the magnesium uptake is affected by carbonate ion concentration (Elderfield et al., 2006), salinity (Ferguson et al., 2008) and growth rate (Elderfield et al., 2002; Ni et al., 2007), Mg isotope fractionation in foraminifera is thought to be unaffected by these processes (Pogge von Strandmann, 2008). Fractionation is also not thought to be influenced by the size or existence of an internally controlled calcium pool, or by kinetic fractionation during aqueous transport (Pogge von Strandmann, 2008; Richter et al., 2006; Wombacher et al., 2011). The effect of temperature, though, is less well constrained, as there are contrasting reports as to whether Mg isotope fractionation during uptake into carbonates is temperature dependent. Some studies report a weak temperature dependence in high-Mg and inorganic calcite (Wombacher et al., 2011; Li et al., 2012; Yoshimura et al., 2011), while analysis of biogenic low-Mg calcite have no reported temperature-dependant fractionation over a temperature range of 5–35 °C (Saulnier et al., 2012; Pogge von Strandmann, 2008; Chang et al., 2004; Wombacher et al., 2011; Saenger and Wang, 2014).

In this study, we undertake to improve our understanding of causes of Mg isotope fractionation in modern foraminiferal species to assess their applicability of in deep time. We then use this information to reconstruct the Mg isotope composition of seawater over the past 40 Myr, in order to constrain Mg cycling in seawater over this period.

2 Materials and methods

2.1 Samples

Core-top samples and species were chosen to expand and complement those reported in the literature to gain better understanding of the processes causing Mg isotope fractionation during uptake into foraminiferal tests. The symbiont-bearing surface dwelling species *Globigerinoides ruber*, *Gs. sacculifer*, *Orbulina universa* and *Gs. conglobatus*, and the asymbiotic thermocline dwellers *Globorotalia tumida*, *G. truncatulinoides* and *G. inflata* were picked, when present, from cores GeoB1206-1, GeoB1208-1 and GeoB5142-2 all in the South Atlantic (Table 1). All of these box corer samples are considered to be Holocene in age. Modern temperatures and salinities were taken from the nearest cell in the ODV representation of the World Ocean Atlas (Table 1). Combined with previous analyses (Pogge von Strandmann, 2008), these provide a sample suite with depth gradients of $>$ 3000 m with similar ($\sim$ 2 °C difference) temperatures, thereby allowing us to address questions on the effect of dissolution on Mg isotope ratios in foraminiferal carbonates.

Cenozoic samples ranging from Eocene to Pleistocene in age were taken from Ocean Drilling Programme Leg 208 Sites ODP 1262, 1263 and 1264 on Walvis Ridge (Table 1). The ages are based on the shipboard age models (Zachos et al., 2004). No single species is available throughout the record and hence we spliced records derived from *O. universa* and *Globigerina venezuelana*. Specimens with minimal overgrowth or diagenetic infilling were selected. Given the very long ($\sim$ 10 Myr) modern ocean residence time of

Table 1. Mg isotope compositions and data from both core-top and past foraminifera.

Core	Species	Size fraction (μm)	Depth (m)	Salinity	SST (°C)	CO_3^{2-} μmol L^{-1}	Mg / Ca mmol/mol	Sr / Ca mmol/mol	Al / Ca μmol L^{-1}	Mn / Ca μmol L^{-1}	δ^{25}Mg (‰)	2 s.e.	δ^{26}Mg (‰)	2 s.e.	Δ^{25}Mg (‰)	Age (Myr)
Core-top foraminifera																
1206-1	*G.tumida*	> 500	940	35.63	19.71	73	1.9	1.28	24	16	−2.58	0.02	−4.95	0.03	0.00	
1208-1	*G.tumida*	> 500	2971	35.57	17.71	108	2.0	1.28	60	12	−2.72	0.01	−5.21	0.01	−0.01	
1211-1	*G.tumida*	> 500	4089	35.57	19.52	90	1.5	1.24	22	9	−2.71	0.03	−5.15	0.02	−0.03	
1206-1	*G.ruber*	> 300	940	35.63	19.71	73	2.6	1.39	29	13	−2.44	0.01	−4.63	0.03	−0.03	
1208-1	*G.ruber*	> 300	2971	35.57	17.71	108	2.6	1.41	49	4	−2.53	0.05	−4.86	0.02	0.00	
1211-1	*G.ruber*	> 300	4089	35.57	19.52	90	2.0	1.37	69	16	−2.4	0.02	−4.65	0.03	0.02	
5142–2	*G.ruber*	> 300	3946	36.8	23.88	93	3.9	1.38	2	2	−2.46	0.01	−4.69	0.02	−0.02	
1206-1	*G.sacculifer*	> 300	940	35.63	19.71	73	3.1	1.35	130	22	−2.6	0.03	−5.01	0.03	0.01	
1208-1	*G.sacculifer*	> 300	2971	35.57	17.71	108	2.8	1.36	49	7	−2.71	0.02	−5.23	0.02	0.01	
1211-1	*G.sacculifer*	> 300	4089	35.57	19.52	90	2.6	1.31	173	25	−2.61	0.02	−4.96	0.03	−0.03	
1206-1	*O.universa*	> 300	940	35.63	19.71	73	4.5	1.39	11	9	−2.56	0.01	−4.93	0.01	0.01	
5142-2	*O.universa*	> 300	3946	36.8	23.88	93	5.4	1.28	38	2	−2.53	0.03	−4.87	0.03	0.01	
1206-1	*G.trunclinoides*	> 300	940	35.63	19.71	73	2.6	1.38	107	34	−2.45	0.04	−4.66	0.04	−0.02	
1206-1	*G.inflata*	> 300	940	35.63	19.71	73	2.2	1.37	58	18	−2.38	0.01	−4.56	0.02	0.00	
5142-2	*G.conglobatus*	> 300	3946	36.8	23.88	93	2.7	1.35	24	4	−2.29	0.01	−4.34	0.02	−0.03	
Sediment foraminifera																
1264B 1H1	*O.universa*	> 300					5.31	1.36	163	11	−2.61	0.03	−4.97	0.02	−0.02	0.06
1264B1H5	*O.universa*	> 300					5.59	1.32	261	23	−2.53	0.01	−4.88	0.02	0.02	1.15
1264A 3H6	*O.universa*	> 300					5.69	1.21	308	42	−2.41	0.02	−4.61	0.03	0.00	4.04
1263A 4Hcc	*G.venezuelana*	> 355					3.02	1.20	54	58	−2.37	0.04	−4.56	0.01	0.01	5.50
1264A 11H6	*O.universa*	> 300					4.49	1.10	128	24	−2.28	0.03	−4.44	0.05	0.03	7.82
1264A 17H6	*O.universa*	> 300					3.91	1.21	289	21	−2.30	0.03	−4.42	0.05	0.00	11.90
1264A17H6	*G.venezuelana*	> 300					2.09	1.21	20	76	−2.24	0.00	−4.30	0.01	0.00	11.90
1264A 18H1	*G.venezuelana*	> 300					1.96	1.23	41	68	−2.32	0.01	−4.42	0.01	−0.02	13.00
1264A18H6	*G.venezuelana*	> 300					2.03	1.24	147	81	−2.16	0.01	−4.14	0.01	0.00	14.10
1264A 19H1	*O.universa*	> 300					3.89	1.16	157	63	−2.29	0.03	−4.34	0.05	−0.02	14.70
1264A 19H1	*G.venezuelana*	> 300					2.28	1.26	94	52	−2.21	0.04	−4.18	0.02	−0.03	14.70
1264A 19H6	*G.venezuelana*	> 300					2.39	1.27	16	33	−2.10	0.01	−4.09	0.01	0.03	17.10
1264A 20H1	*G.venezuelana*	> 300					2.15	1.26	225	28	−2.15	0.03	−4.11	0.04	−0.01	18.20
1264A 20H7	*G.venezuelana*	> 300					3.48	1.19	175	60	−2.14	0.02	−4.10	0.01	0.00	18.80
1264A 21Hcc	*G.venezuelana*	> 355					2.05	1.25	10	22	−2.20	0.03	−4.22	0.01	0.00	21.30
1264A 24cc	*G.venezuelana*	> 300					2.54	1.16	43	54	−2.26	0.02	−4.30	0.03	−0.02	23.01
1264B26Hcc	*G.venezuelana*	> 355							22	24	−2.45	0.01	−4.75	0.02	0.02	25.10
1264A26Hcc	*G.venezuelana*	> 355					2.87	1.28	155	29	−2.45	0.03	−4.65	0.01	−0.03	25.80
1264A 27cc	*G.venezuelana*	> 300					2.19	1.38	273	34	−2.37	0.01	−4.57	0.04	0.01	26.25
1264A 29Hcc	*G.venezuelana*	> 355					2.78	1.30	38	69	−2.24	0.01	−4.31	0.01	0.01	29.70
1264B 29Hcc	*G.venezuelana*	> 355					2.77	1.22	41	52	−2.20	0.05	−4.22	0.02	0.00	29.70
1263A 11Hcc	*G.venezuelana*	> 355					2.43	1.26	32	48	−2.16	0.02	−4.12	0.04	−0.02	35.40
1263B 6Hcc	*G.venezuelana*	> 300					2.55	1.28	53	13	−2.20	0.01	−4.21	0.01	0.00	36.70
1263A 14hcc	*G.venezuelana*	> 355					2.30	1.28	169	16	−2.11	0.02	−4.09	0.05	0.02	40.50

Mg (Berner and Berner, 1996), sampling resolution was ∼ 5 Myr overall, with up to 1 Myr resolution across the middle Miocene when other isotope systems, such as Li, show major changes which have been related to weathering (Misra and Froelich, 2012).

Assuming that the Mg isotope fractionation from seawater stays constant for individual species through time, our data set allows us to splice together data from *O. universa* from 0 to 14.7 Ma, and from *G. venezuelana* from 5 to 40 Ma. We assessed for possible offsets between these species by analysing them from the same samples (1264A 17H6 and 19H1, as well as core-top samples for *O. universa*). The variability in δ^{26}Mg in core-top *O. universa* from this study and Pogge von Strandmann (2008) is ±0.18 ‰ (2 SD), and combined with the analytical uncertainty of δ^{26}Mg in modern seawater (±0.06 ‰, 2 SD, Foster et al., 2010) as well as the foraminifer samples themselves (0.01–0.14 ‰) gives a compound uncertainty of ±0.21 ‰ on the correction factors applied.

2.2 Methods

Our methods of cleaning and chemical purification of foraminiferal carbonate have been published in detail elsewhere (Pogge von Strandmann, 2008). Briefly, ∼ 20 tests were picked per sample, crushed and cleaned in methanol and 18.2 MΩ H_2O to remove clays, followed by heating with ammonia buffered with 1 % H_2O_2 to remove organics. The samples were then split, with ∼ 50 % taken for trace element analysis on an Element 2 Sector ICP-MS (inductively coupled plasma mass spectrometer), with samples matrix matched against multi-element standards produced from individual high-purity single element standards, with an intercalibrated in-house standard (BSGS, Ni et al., 2007), and the international carbonate reference standard JLs-1 as assessments of accuracy. These analyses are necessary not only to acquire elemental ratios important for interpretation (e.g. Mg / Ca), but also to determine whether silicate clays have been sufficiently removed to not affect Mg isotope ratios. Many clays contain high-Mg abundances with isotope ratios significantly different from that of carbonate, and hence clay content was assessed by determining Al / Ca

and Mn / Ca ratios (Pogge von Strandmann, 2008). Low Al and Mn abundances are the main reason 50 % of the sample was dedicated to concentration analyses. Low Al / Ca (< 300 µmol mol^{-1} (Pogge von Strandmann, 2008), where most samples < 50 µmol mol^{-1}l) and Mn / Ca and a lack of a positive correlation between Al / Ca or Mn / Ca and Mg / Ca or δ^{26}Mg show that silicate clays or Fe-Mn coatings are not a source of Mg in these analyses.

The other ~ 50 % of sample was purified for Mg isotopes using our previously described method of cation exchange columns (AG-50W X-12) using 2.0M HNO_3 as an elution agent (Foster et al., 2010; Pogge von Strandmann, 2008; Pogge von Strandmann et al., 2011, 2012). Purified samples were analysed for Mg isotopes using a Finnigan Neptune multi-collector ICP-MS, with an Elemental Scientific Apex-Q "moist" plasma introduction system. This system has the same benefits as the "wet" plasma quartz spray chambers commonly used for Mg isotopes (suppression of C_2^+ and CN^+ interferences and no significant hydride formation) but also higher sensitivity (~ 100 pA of $^{24}Mg^+$ for a 50 ng mL^{-1} solution at an uptake rate of 50 µL min^{-1}) (Pogge von Strandmann et al., 2011). The total procedural blank of this method is ~ 0.2–0.25 ng, which is insignificant compared to the mass of sample used. Analytical precision and accuracy were assessed by multiple analyses of seawater, yielding $\delta^{26}Mg = -0.82 \pm 0.06$ ‰ (2 SD, n =26, Foster et al., 2010). Analytical precision on carbonate was assessed by repeated (including diluted) analyses of coral carbonate detailed in Pogge von Strandmann (2008) (-3.44 ± 0.08 ‰, n =13, 2 SD).

2.3 Modelling seawater Mg using Mg isotopes

A record of seawater δ^{26}Mg gives a possibility of attempting to reconstruct Mg sources and sinks, as well as seawater Mg concentrations. In addition, constraining past riverine Mg fluxes and isotope ratios could provide constraints on changes in weathering and the related atmospheric CO_2 withdrawal. A series of assumptions must be made about Mg behaviour during this time, resulting in two models that define endmember scenarios. For our first model (termed "fixed sink" model), we assume that the hydrothermal Mg sink is proportional to the mid-ocean ridge spreading rate, taken from the GEOCARB II model (Berner, 1994). The dolomite sink is constrained from rates of shallow water carbonate accumulation (Holland and Zimmermann, 2000; Hay, 1994), on the assumption that such carbonate is predominantly dolomitised. Removal onto low-temperature clays is thought to be minimal, with very poor constraints on any isotope fractionation (Tipper et al., 2006b), and are therefore ignored for this model. Given that the isotope fractionation caused by these sinks is reasonably well constrained (Higgins and Schrag, 2010b), this leaves the river Mg flux and isotope ratio as remaining unknowns. For the riverine flux, we use the Sr riverine flux calculated from foraminiferal Sr / Ca and

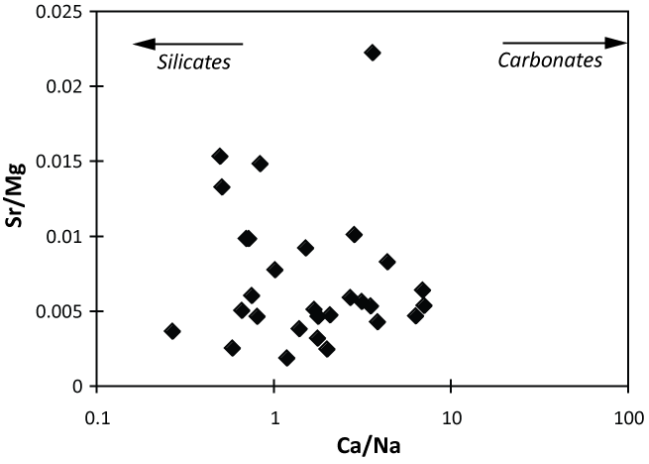

Figure 1. Mg / Sr and Ca / Na from the Earth's major rivers (Gaillardet et al., 1999), showing that Mg / Sr does not vary between carbonate (high Ca / Na) and silicate (low Ca / Na) weathering, allowing use of riverine Sr fluxes (Lear et al., 2003) to calculate river Mg fluxes. Rivers with high Mg / Sr (Rhone, Huanghe, Wisla, Rhine) plausibly have anthropogenic contamination.

$^{87}Sr / ^{86}Sr$ ratios (Lear et al., 2003; McArthur et al., 2001). The relationship between Mg and Sr in rivers is relatively straightforward, and there is little change in Sr / Mg for rivers draining silicate or carbonate terrains (Fig. 1, Gaillardet et al., 1999). Hence the modern global river Sr / Mg ratio and the riverine flux over the past 40 Myr are used to calculate the 40 Ma riverine Mg flux.

The seawater Mg budget N is calculated by $dN / dt = F_R - F_{MOR} - F_{SED}$, where F is the flux from rivers, mid-ocean ridges and sedimentation, given in mol/yr. The isotope ratios are then calculated from the standard mass-balance formula:

$$N\frac{dR_{SW}}{dt} = F_r(R_r - R_{SW}) - F_{MOR}(R_{MOR} - R_{SW}) - F_{sed}(R_{sed} - R_{SW}). \quad (1)$$

The isotope ratio R of the sinks is calculated from the equation $\Delta_{sink} = R_{sink}$-R_{SW}, where removal at MOR is thought to be quantitative, resulting in no isotope fractionation, and $\Delta_{sed} \sim 1.7$ ‰ for dolomite (Tipper et al., 2006b; Higgins and Schrag, 2010b). The equations were then solved in 100 000 year time slices, using the seawater δ^{26}Mg values calculated from the foraminiferal record (see below), and solving for the isotope ratio of river water.

The second main model allows the flux of Mg to dolomite to be a variable ("fixed source" model). Rather than simply solving the flux mass balance, the isotope mass balance equation is solved for F_{sed}, using the same assumptions for the hydrothermal flux and riverine flux as in the first model. This then requires a "known" riverine isotope ratio through time, which is constrained from the river $^{87}Sr / ^{86}Sr$ of Lear et al. (2003), on the assumption that the river Sr isotope ratio is dominantly controlled by mixing

between weathering of carbonate ($^{87}Sr/^{86}Sr$=0.708) and silicate ($^{87}Sr/^{86}Sr$=0.722) endmembers. This allows calculation of the δ^{26}Mg of rivers, by assuming that these endmembers dominantly control the δ^{26}Mg of modern rivers (flux-weighted mean -1.09 ± 0.05 ‰, Tipper et al., 2006b), and back-calculating to the δ^{26}Mg of the carbonate (δ^{26}Mg= -1.45 ‰) and silicate (δ^{26}Mg= -0.2 ‰) endmembers. This approach requires that Mg isotope fractionation due to silicate secondary mineral formation is relatively less important than that caused by variations in lithology (e.g. Tipper et al., 2008). Clearly, this approach also assumes that Sr isotopes are not anomalously influenced by radiogenic Himalayan carbonates (Palmer and Edmond, 1992), although it has been suggested that the radiogenic Himalayan flux is due to mixing between unradiogenic carbonate and radiogenic silicate weathering (Galy et al., 1999). In any case, as will be shown below, these changes are a relatively minor unknown variable in the Mg system.

3 Results

To assess potential diagenesis and/or recrystallisation, Sr / Ca ratios were examined in both modern and ancient foraminifera. In the core-top samples, Sr / Ca from *G. ruber* and *G. sacculifer* were identical to the range of other pristine foraminifera (Ni et al., 2007). The Eocene–Holocene samples have similar Sr / Ca ratios (1.19–1.3 mmol/mol, compared to core-top 1.24–1.41 mmol mol^{-1}; Table 1), which are higher than the Sr / Ca range thought to characterise diagenetically altered and re-crystallised foraminifera ($> \sim 1.2$ mmol mol^{-1}, Kozdon et al., 2013). Mg / Ca ratios in foraminifera from this study are also generally lower than those ratios thought to represent diagenesis ($> \sim 5.5$ mmol mol^{-1}, Kozdon et al., 2013).

On average, Mg / Ca temperatures calculated from the core-top samples using species-specific calibration equations (Anand et al., 2003) are within 0.7 °C of the recorded sea surface temperature (SST). There are no overall resolvable correlations between δ^{26}Mg and Mg / Ca (Fig. 2a) or with depth (i.e. dissolution) or CO_3^{2-} concentrations. For the latter, *G. ruber* and *Gt. tumida* show an apparently negative trend, which is, however, not truly resolved within the analytical uncertainty of the methodology for δ^{26}Mg (Fig. 2c). Mg isotope ratios of *G. truncatulinoides*, *G. sacculifer* and *G. ruber* are within the range of previous studies (Chang et al., 2004; Pogge von Strandmann, 2008; Wombacher et al., 2011). The new data for *G. inflata* are similar to *G. truncatulinoides*, its nearest relative in the study with the most similar habitat. *G. conglobatus* records values more positive than the overall foraminifer average and also more positive than the other species in the genus, *G. sacculifer* and *G. ruber*. The new δ^{26}Mg values for *O. universa* and *G. tumida* have expanded the range of the previously published data set for those species (Fig. 3). The average for

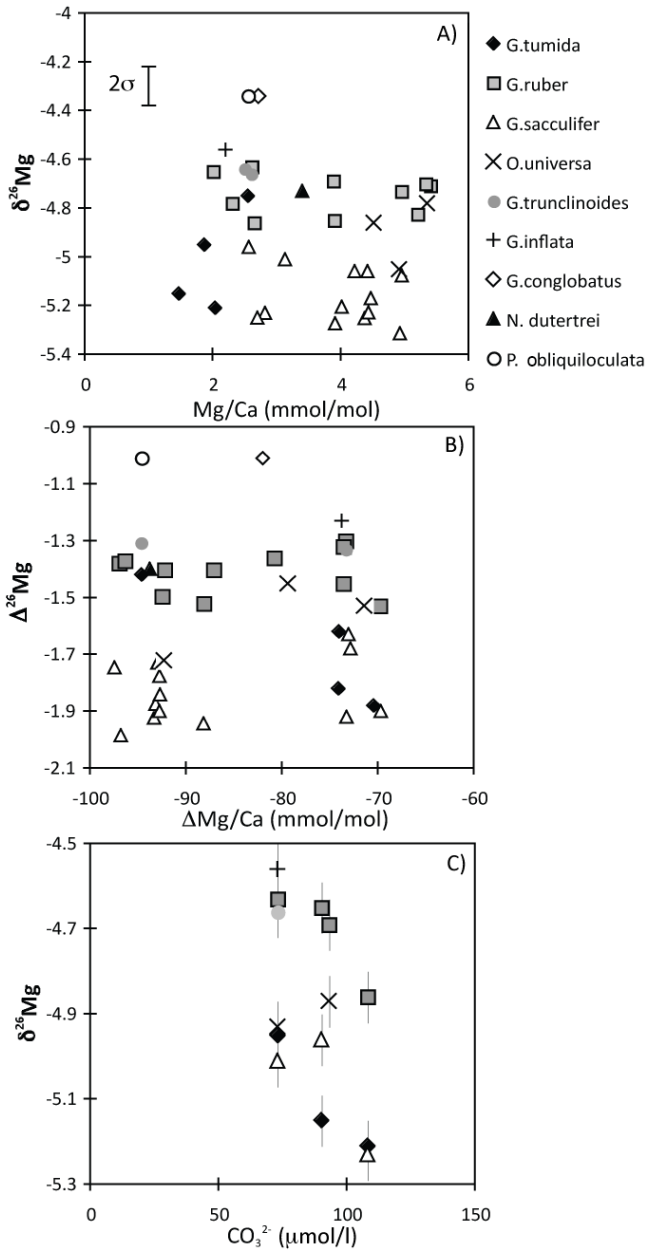

Figure 2. (a) Mg / Ca ratios vs. δ^{26}Mg of all species analysed (including from Pogge von Strandmann, 2008). No relationship exists between these two factors. **(b)** The Mg / Ca and δ^{26}Mg fractionation after inorganic calcification (temperature-dependent for Mg / Ca) has been removed, showing the extent of biologically controlled impacts on magnesium and its isotopes in foraminifers. **(c)** Relationship between δ^{26}Mg and carbonate ion concentration. The error bars represent external uncertainty (2 SD), to demonstrate that the potential relationships hinge on single data points.

δ^{26}Mg in low-Mg foraminifera from this study and others (Pogge von Strandmann, 2008; Wombacher et al., 2011) is -4.62 ± 0.67 ‰ (2 SD), with the main outliers from the

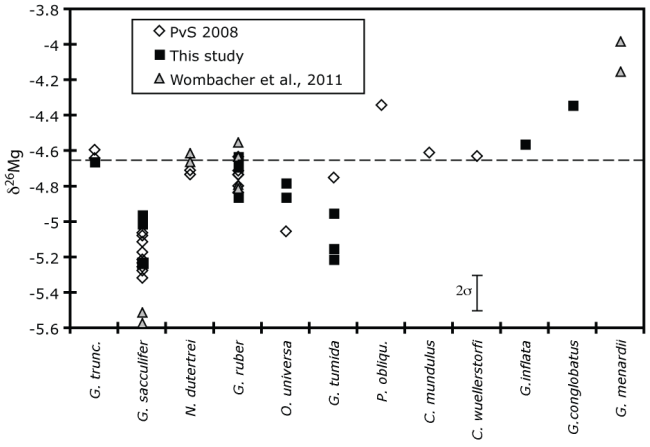

Figure 3. A compilation of Mg isotope data (Pogge von Strandmann, 2008; Wombacher et al., 2011) from low-Mg planktonic foraminifera. Data from Chang et al. (2004) are not included, due to the lack of a data table in that publication. The dotted line represents the average of the data.

average being *G. sacculifer* (≤ 0.95 ‰ lighter than average) and *G. menardii* (≤ 0.64 ‰ heavier than average) (Fig. 3).

The Eocene–Holocene samples show a decrease at ~ 14 Ma from -4.14 ‰ to the present day. For most of the time between the middle Eocene and middle Miocene, values are approximately constant at -4.3 ‰, aside from several isotopically light data points in the late Oligocene (Fig. 4a).

4 Discussion

4.1 Mg incorporation in foraminifera – a window into biomineralisation

Little is as yet understood about the incorporation of Mg into foraminiferal calcite, and in particular on the associated Mg isotope fractionation. This study strengthens the information on species-dependent variability in Mg isotope fractionation (Fig. 3), reiterating that a clear understanding of the controls on Mg isotope fractionation may yield important clues for the incorporation of Mg into tests and hence ultimately the process of biomineralisation. Test growth rate and seawater calcite saturation state have previously been shown not to affect test δ^{26}Mg values (Pogge von Strandmann, 2008). Several studies have established that δ^{26}Mg in planktonic foraminifera does not appear to be dependent on calcification temperature (Chang et al., 2004; Pogge von Strandmann, 2008; Wombacher et al., 2011), in contrast to a weak temperature dependence of δ^{26}Mg in calcitic sclerosponges and corals (Wombacher et al., 2011; Yoshimura et al., 2011). The greatest δ^{26}Mg variation in this study's *G. ruber* and *G. sacculifer* is indeed in samples with almost identical SST.

Consequently, there is no correlation between δ^{26}Mg and Mg / Ca (Fig. 2a). This suggests that the active removal or

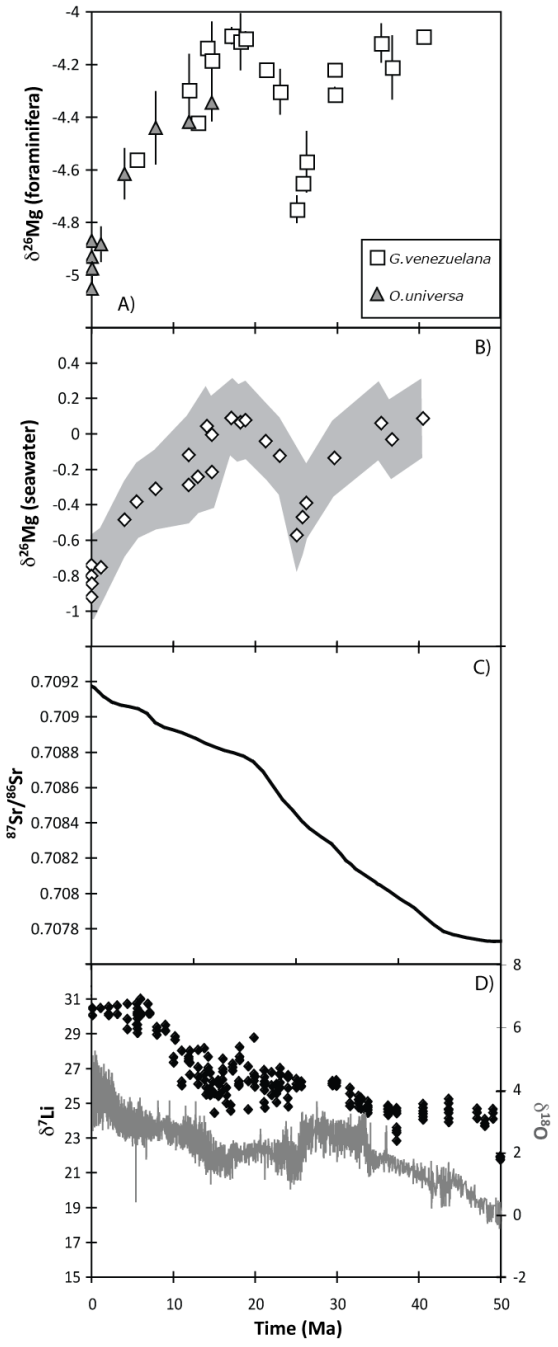

Figure 4. (a) Foraminiferal δ^{26}Mg values from the past 40 Myr. Uncertainty on the age model is smaller than the symbol size. The error bars represent the 2 SD analytical reproducibility of the individual samples. **(b)** Reconstructed seawater δ^{26}Mg from the foraminiferal record. The grey band shows the extent of uncertainty, including analytical uncertainty and scatter due to the spread in modern *O. universa* and the offset between the two analysed species (± 0.28 ‰). **(c)** LOWESS Cenozoic Sr isotope data (McArthur et al., 2001) **(d)** Li (Black diamonds) and O (grey line) isotope ratios of planktonic foraminifera (Misra and Froelich, 2012; Zachos et al., 2001).

biocomplexation of Mg, to allow for calcite growth, or the enrichment of Ca by active pumping, does not preferentially discriminate by a constant fractionation factor against heavy Mg isotopes, either for individual species, or for planktic foraminifera as a whole. It seems likely, however, that the processes that dramatically reduce the Mg concentrations of foraminiferal tests relative to inorganic calcite are the same that drive the Mg isotope composition of the tests significantly lighter than inorganic calcite. Given that the Mg isotope ratio of seawater is well known (-0.82 ± 0.06 ‰, Foster et al., 2010), and that the thermodynamics and fractionation during the precipitation of inorganic carbonate is reasonably well constrained (Δ^{26}Mg ~ 2.6 ‰ at 20 °C, Busenberg and Plummer, 1989; Mucci, 1987; Galy et al., 2002; Pogge von Strandmann, 2008; Wombacher et al., 2011; Hippler et al., 2009; Immenhauser et al., 2010), other effects must account for a $\Delta^{26}Mg_{foram\text{-}inorg\,cc}$ of -0.55 to -2.1 ‰ , which is the isotopic difference between inorganic calcite precipitated from seawater (at a given temperature) and the value measured in the foraminiferal tests.

It has been proposed that Mg is reduced by active pumping out of an intra-cellular vacuole with a seawater starting composition (Bentov and Erez, 2006: Erez, 2003; de Nooijer et al., 2014). Hence, the Mg isotope fractionation could be the result of this pumping, which would be expected to follow a Rayleigh-type isotope fractionation process, with slightly greater fractionation at lower temperature, which however is not observed (Wombacher et al., 2011; Pogge von Strandmann, 2008). Calcification from this modified solution would then be an inorganic calcification process (Pogge von Strandmann, 2008). However, no mechanism for active Mg removal has yet been identified. In addition, the wide ranges in Mg / Ca fractionation caused by the "vital-effect" (ΔMg / $Ca_{foram\text{-}inorg\,cc}$, which is the difference between the Mg / Ca of inorganic calcite at a given temperature and seawater composition and that measured in the foraminiferal tests) at relatively small variation in $\Delta^{26}Mg_{foram\text{-}inorg\,cc}$ (again corrected for inorganic fractionation) imply that no single process is responsible for both the removal of Mg, and the discrimination against heavy Mg isotopes (Fig. 2b).

Another possible process is active pumping of Ca, via Ca pumps, from vacuolisation of seawater into the Ca reservoir, rather than removal of Mg from the Ca reservoir (Raitzsch et al., 2010; ter Kuile, 1991), thereby changing the Mg / Ca ratio. Nehrke et al. (2013) suggest that Ca for test calcification is primarily supplied by a combination of active trans-membrane transport, which has been shown to strongly discriminate against other elements due to differences in surface charge density, and passive transport (i.e. vacuolisation) (Nehrke et al., 2013). In this model, most of the Ca is supplied by trans-membrane transport, which strongly discriminates against Mg, combined with a relatively small amount passive transport, which adds Mg in seawater-like proportions. Hence if trans-membrane transport favours light Mg isotopes, which may be more energetically favourable, then the variability in δ^{26}Mg and Mg / Ca could be explained by either species-specific across-membrane Ca transport mechanisms (which are variably efficient in discriminating against Mg, or, in other words, incorporates some Mg as a by-product during Ca transport), or species-specific amounts of passive transport of seawater (Nehrke et al., 2013).

The Nehrke et al. (2013) model suggests that trans-membrane transport is the same for coccolithophores (with very low Mg / Ca) and foraminifera (with higher Mg / Ca), and thus in both cases trans-membrane transport initially yields tests with low Mg / Ca. Subsequently, for foraminifera, passive transport of seawater increases Mg / Ca, creating the difference between coccolithophores and foraminifera. However, given that coccolithophores have Mg isotope ratios similar or higher than inorganic calcite (i.e. lower than seawater, but significantly higher than foraminifera) (Wombacher et al., 2011; Ra et al., 2010), this combined model cannot explain why foraminifera have such low δ^{26}Mg relative to coccolithophores.

It is possible that the benthic foraminifera (*A. aomoriensis*) examined by Nehrke et al. (2013) has different calcification mechanisms than planktic ones, although available data for deep sea benthic foraminifera have similar ratios to planktic ones (Pogge von Strandmann, 2008). Importantly, *A. aomoriensis* is a brackish water rather than open ocean species, which might have acquired a different calcification mechanism to deal with the different environmental conditions. In addition, if passive addition of seawater caused the variability in foraminifer Mg / Ca, then a correlation would be expected between the "organic" Mg / Ca (i.e. ΔMg / $Ca_{foram\text{-}inorg\,cc}$) and δ^{26}Mg fractionation, because Mg would stem from the same reservoir (seawater), which, however, is not observed (Fig. 2b). Hence Mg isotopes suggest that coccolithophores and foraminifera have different Ca transport mechanisms, with different efficiency with regard to discrimination against Mg. Passive addition of seawater could explain why high-Mg foraminifera (*Cycloclypeus* sp. and *Marginopora* sp.) have higher δ^{26}Mg than low-Mg foraminifera (Yoshimura et al., 2011; Wombacher et al., 2011), because both Mg / Ca and δ^{26}Mg are then closer to seawater, but this needs to be experimentally verified.

Our findings suggest that Mg isotopes can provide a further insight into calcification mechanisms. Future models into controls on Mg / Ca need to consider Mg and Ca isotope, as well as elemental, fractionation. However, the relatively narrow δ^{26}Mg range exhibited by individual species (*G. sacculifer*: ~ 0.6 ‰, *G. tumida*: ~ 0.5 ‰, *G. ruber*: ~ 0.3 ‰), and the lack of apparent control by environmental parameters, suggests that changes larger than ~ 0.5 ‰ in the past indicate changes in the seawater Mg isotope values. However, equally, these data demonstrate the importance of a calibrated, single-species approach, given that the δ^{26}Mg variation seen in core-top foraminifera of different species is

that same as that observed across the past 40 Myr in a single species.

4.2 A Cenozoic seawater reconstruction based on foraminiferal calcite

The δ^{26}Mg values calculated for seawater for the past 40 Myr are clearly resolvable from present-day ratios, and suggest that seawater δ^{26}Mg was ~ 0 ‰ during the middle Eocene (Fig. 4). For most of the time between the middle Eocene and middle Miocene, seawater had approximately constant δ^{26}Mg, aside from an approximately 10 Myr decrease in isotope ratios in the late Oligocene, with the δ^{26}Mg minimum coinciding with the late Oligocene warming trend (Zachos et al., 2001). From the middle Miocene (< 14 Ma), seawater δ^{26}Mg begins to decrease sharply.

Given its residence time of ~ 10 Myr, this strongly suggests that Mg in the modern oceans is not in steady state (Vance et al., 2009), but is evolving rapidly to more negative δ^{26}Mg values. The lack of steady state is supported by data inferred from fluid inclusions in halite, as well as from Sr and Mg isotope ratios in pore fluids, which suggest that the Mg concentration in seawater over the last 40 Ma has been increasing, with a gradient that is becoming steeper towards the present (Holland and Zimmermann, 2000; Zimmermann, 2000; Fantle and DePaolo, 2006; Higgins and Schrag, 2012).

There are likely two dominant controls on both the Mg concentration and isotope ratios in the oceans: the riverine input and removal into dolomite. Removal into low-temperature clays formed during alteration of oceanic basalt may also be a sink of oceanic Mg. However, estimates of this flux in the present day are highly variable (7–80 % of the dolomite sink, Elderfield and Schultz, 1996; Holland, 2005; Tipper et al., 2006b), and no Mg isotopic constraints exist. Although reconstructing the flux of any element is highly complex, and no unequivocal riverine flux record has ever been constructed, the river elemental fluxes have likely been highly variable over the past 40 Myr, due to changes in glaciation, orogeny, plant evolution, etc. (Li et al., 2009a; Li and West, 2014; Wanner et al., 2014). The Mg isotope ratio of rivers (present global flux-weighted mean ~ -1.09 ‰, Tipper et al., 2006b) will dominantly depend on the ratio of carbonates (δ^{26}Mg ~ -5 to -1 ‰) to silicates (-0.25 ± 0.1 ‰) in the catchment area (Pogge von Strandmann et al., 2008, 2012; Tipper et al., 2006a, b, 2008, 2010, 2012; Li et al., 2010; Teng et al., 2010b). Interestingly, the overall decrease in seawater δ^{26}Mg appears to start around 15 Ma, which is also when Li isotopes start increasing (Fig. 4d), which has been interpreted as a decrease in the congruency of continental weathering (Misra and Froelich, 2012), and it is possible that the process which caused this change in congruency also affected the δ^{26}Mg of rivers. The δ^{26}Mg decrease could also be coupled to the decrease in global temperatures and build-up of ice-sheets (Zachos et al., 2001; Lear et al., 2000). It is unlikely that changes in the calcium compensation depth will have resolvedly affected Mg isotopes in the Cenozoic as dolomite is predominantly a shallow-water carbonate, and therefore is always likely to have existed above the CCD.

In previous attempts to model Mg concentrations in the ocean (Holland, 2005), the river flux has been kept constant over the entire 35 Myr period, which is unlikely to reflect reality given the large climatic variability during this time (e.g. Zachos et al., 2001). However, Holland (2005) suggests that climate was not important, because the removal of Mg into dolomite is the main factor controlling seawater concentrations. The formation rate of dolomite has varied significantly during the course of the Cenozoic; dolomite deposition is thought to have accounted for $\sim 3.8 \times 10^{12}$ mol yr^{-1} Mg at 35 Ma (Holland, 2005), and estimates for the modern removal are between ~ 0.2–1.7×10^{12} mol yr^{-1} (Elderfield and Schultz, 1996; Tipper et al., 2006b; Holland, 2005). Factoring in minor changes in the Mg sink at mid-ocean ridges, this significant decrease of the removal of Mg into dolomites is thought to have led to a considerable increase in the Mg concentration of the oceans, resulting in Mg being out of steady state. The effects of a variable hydrothermal sink, as proposed by some studies, is discussed below.

The seawater Mg concentrations from both endmember models used in this study significantly increase towards the present day, and are very similar to models of seawater Mg based on the chemistry and ^{87}Sr / ^{86}Sr (Fantle and DePaolo, 2006) and on the δ^{26}Mg (Higgins and Schrag, 2012) of deep-sea carbonate pore fluids (Fig. 6e). Overall, these models yield somewhat lower Mg than amounts inferred from ridge axis carbonate veins (Coggon et al., 2010; Horita et al., 2002; Zimmermann, 2000), which tend to suggest a more gradual slope (Fig. 6e).

Because rivers are the dominant source of Mg to the oceans, both their flux and isotopic compositions influence the seawater δ^{26}Mg. Hence, the modelled riverine flux and δ^{26}Mg cannot be kept constant throughout the studied time period. Figure 5 shows the effect of constant modern-day values for the riverine flux and isotope ratio on seawater δ^{26}Mg, using published values for the dolomite and hydrothermal Mg sinks (see "fixed sink" model description in Sect. 2.3; Figs. 5 and 6). Importantly, a fixed riverine flux and isotope composition cannot reproduce the observed pattern. Varying the riverine flux, based on estimates from Lear et al. (2003), shows that although the general trends in seawater δ^{26}Mg are followed, changes of the riverine δ^{26}Mg are required to more accurately reconstruct the seawater trends (Fig. 5). These changes are fairly large, varying between -3 and $+0.5$ ‰, which is approximately the modern range of rivers (Pogge von Strandmann et al., 2008; Tipper et al., 2006b, 2008, 2012; de Villiers et al., 2005; Huang et al., 2012; Wimpenny et al., 2011). However, given that the dominant control over the δ^{26}Mg of rivers is the lithology undergoing weathering (isotopically light carbonates, and heavy silicates), this would require that during most of the Oligocene and late Miocene rivers, were dominated by carbonate weathering,

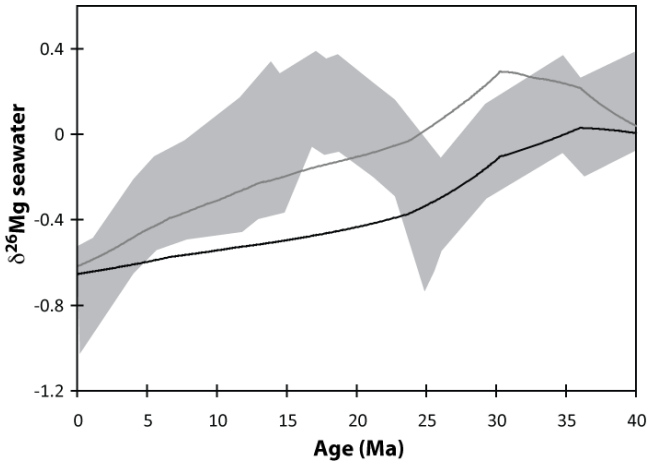

Figure 5. Model showing the effect on the fixed sink model when the river flux and isotope ratios are held constant at modern values (black line), and when only the riverine isotope ratios are held constant (grey line – river flux derived from Lear et al., 2003; see text for details). The grey field represents the seawater record derived from foraminifera.

and, for the time between the early Miocene glaciation and the Miocene climatic optimum, were dominated by an isotopically very heavy source. Hypothetically, mid-Miocene growth of the East Antarctic ice sheet may have lowered sea level (Zachos et al., 2001; Shackleton and Kennett, 1975; John et al., 2011), and exposed shallow marine carbonate platforms to chemical weathering (Li et al., 2009b). Reconstructions of riverine Sr isotopes during this time, though, do not show such endmember compositions (Galy et al., 1999; Oliver et al., 2003; Palmer and Edmond, 1992; Lear et al., 2003). Equally, high solid rock δ^{26}Mg values (up to +1 ‰) have been reported in heavily weathered rocks, loess and saprolites (Pogge von Strandmann et al., 2008; Teng et al., 2010b; Li et al., 2010). It has, however, also been shown that generally rivers draining such rocks tend to have lower δ^{26}Mg (Tipper et al., 2012). This suggests that an isotopically heavy global river composition must either be due to the formation of significant amounts of (isotopically light) carbonate on the continents, or weathering and destabilisation of previously weathered, secondary clay-rich material, either of which are unlikely to have occurred on a global scale. Hence it seems unlikely that the "fixed sink" model reproduces Mg sources and sinks accurately, and that riverine δ^{26}Mg did not vary by that amount.

The "fixed source" model (assuming river fluxes and isotope ratios based on Sr isotopes (Lear et al., 2003) and the same hydrothermal flux as in the previous model) allows the dolomite sink to be a variable in controlling the δ^{26}Mg of seawater. If lithology is the main controlling factor on river isotope ratios (deconvolved from Sr isotopes based on two endmember mixing), then this suggests that global river δ^{26}Mg has changed relatively little (varying between −0.98 and −1.22 ‰). This seems a more useful approach than the previous model's conclusion of an order of magnitude more variation in river δ^{26}Mg, given that large changes in the isotope ratio of a major element in rivers would require drastic differences in the weathering system.

The fraction of the Mg sink attributed to dolomite relative to hydrothermal uptake (f_{dol}) varies between ∼ 0.1 and ∼ 0.65 (Fig. 6a), with lowest values at the present day and between ∼ 25–30 Ma, and highest values between the early Miocene glaciation and Miocene climatic optimum. This model appears to demonstrate a more realistic approach to the Cenozoic Mg budget: Mg removal by dolomite across the Cenozoic ($0.2 - 3.7 \times 10^{12}$ mol yr^{-1}) is within estimates by other studies. In addition, the seawater δ^{26}Mg decrease starting at ∼ 15 Ma (based on the foraminiferal record) suggests that the modern dolomite sink is at the lower end of estimates from other studies, but agrees well with the only other estimate based on Mg isotopes (Tipper et al., 2006b). The overall pattern of the modelled dolomite removal flux agrees well with Cenozoic estimates of rates shallow-water vs. deep-water carbonate accumulation (with the former predominantly dolomite), which also show a minimum between 25 and 30 Ma, and a rapid decrease from ∼ 20 Ma towards the present day (Hay, 1994; Opdyke and Wilkinson, 1988). Seafloor production rates, and therefore likely the hydrothermal sink, are the matter of some debate. Our models use the estimates from GEOCARB II (Berner, 1994) (Fig. 6b), because these were used by the model of riverine Sr (Lear et al., 2003). However, other estimates suggest a 4–15 % decrease over that past 20 Myr (Coltice et al., 2013; Conrad and Lithgow-Bertelloni, 2007; Muller et al., 2008). The modelled effect of a monotonic 15 % decrease in the hydrothermal flux over the past 20 Myr is ≤ 0.02 ‰ on δ^{26}Mg (due to the lack of isotopic leverage the hydrothermal sink exerts), and a ∼ 6 % increase in N_{Mg}. A 15 % step change at 20 Ma would cause a ∼ 12 % increase in N_{Mg} by the present day. Given the long ocean residence time of Mg, and hence its buffered response, the implication of this is that the increase in seawater Mg concentrations over the past 10–15 Myr was dominantly driven by a combination of increasing riverine flux and decreasing dolomite formation (Fantle and DePaolo, 2006), and not as significantly by a decrease in the hydrothermal sink. This conclusion is tempered by the assumptions inherent in our endmember models, and it is possible that the, as yet unconstrained, low-temperature off-axis Mg sink may have an effect.

If the mean global riverine δ^{26}Mg is controlled by lithology, and therefore can be estimated from Sr isotopes, then our models imply that dolomite formation (as suggested by Holland, 2005) and the river Mg flux are the dominant controls on the Mg isotope ratio seawater, and hence, by implication, its concentration. The endmember models suggest that the oceans are less sensitive to changes in the hydrothermal flux and river isotope ratio, due to the lack of leverage they exert on seawater Mg isotopes, and therefore the coupled Mg

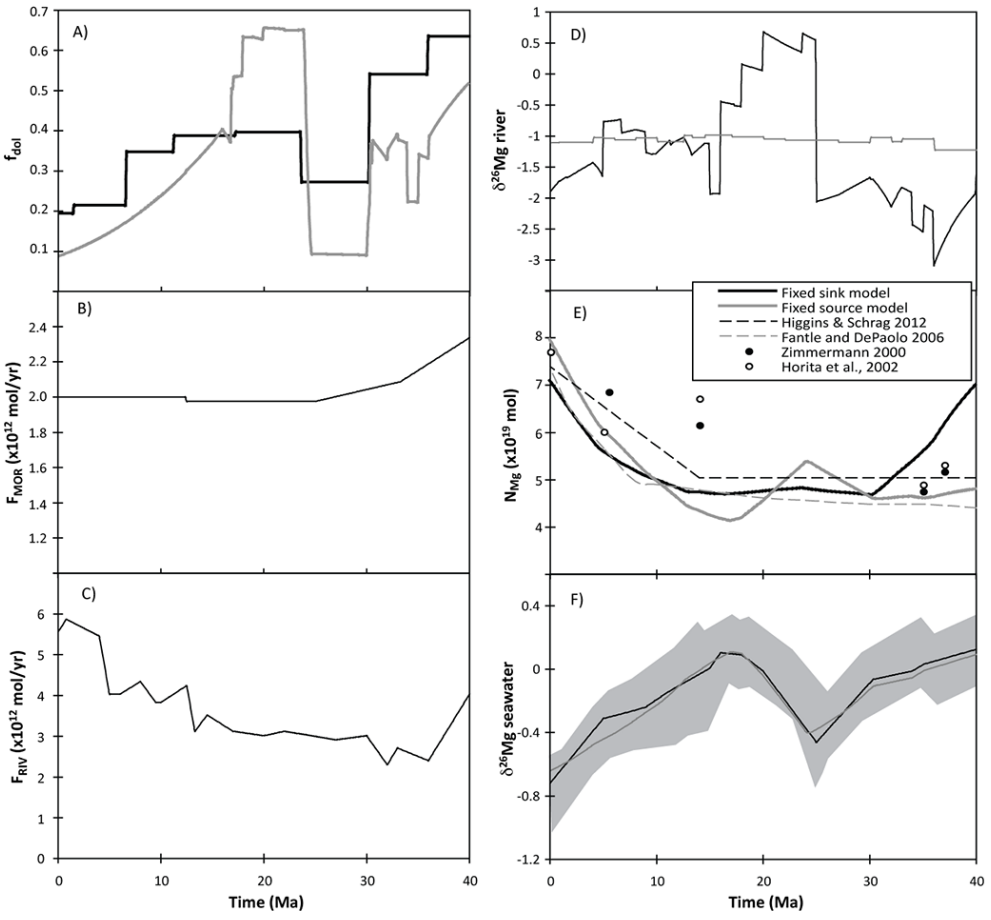

Figure 6. The inputs and outputs from the models (grey line: fixed source model, black line: fixed sink model). **(a)** Fraction of Mg removed by dolomite, relative to that hydrothermal removal. Due to the relative flatness of the hydrothermal flux at 30 Ma, the Mg removal flux by dolomite is essentially parallel to these curves. **(b)** Mg removal flux at mid-ocean ridges, from estimates of past spreading rates. Both models use these values. **(c)** riverine input flux, which is identical for both models. **(d)** Riverine δ^{26}Mg. The fixed sink model derives the river δ^{26}Mg from the isotope mass balance equation, while the fixed source model derives it from the riverine $^{87}Sr/^{86}Sr$ (Lear et al., 2003). **(e)** Model output seawater Mg reservoir. The dashed lines represent other models (Fantle and DePaolo, 2006; Higgins and Schrag 2012) based on pore waters, and the data points are inferred seawater concentrations from fluid inclusions. **(f)** Model results for the seawater δ^{26}Mg. The grey band represents the same uncertainty on the seawater δ^{26}Mg reconstruction as in Fig. 4b.

concentrations, which in any case are relatively buffered due to the long residence time. Interestingly, seawater Li isotopes are thought to have begun a rapid increase towards heavier values from the mid-Miocene climatic optimum at $\sim$ 14 Ma (Fig. 4d), possibly due to a shift in the weathering regime to a more incongruent, weathering-limited system (Misra and Froelich, 2012). Lithium isotope ratios respond only to silicate weathering (Kisakürek et al., 2005; Millot et al., 2010), and therefore there can be no direct link between the concurrent increase in seawater δ^{7}Li and δ^{18}O and the decrease in δ^{26}Mg. This suggests that the overall control, at least from the mid-Miocene onwards, is the climatic cooling trend, which affected both the weathering regime and dolomite formation. The model also suggests a rapid decline in Mg taken up by dolomite at the same time as climate cooled in the early–mid-Oligocene, either due to the cooling, or due to a decrease in the cations supplied from the continents.

5 Conclusions

Foraminifera from core-tops and from the past 40 Myr have been analysed for Mg isotope ratios. Core-top foraminifera show no relationship between δ^{26}Mg, Mg / Ca ratios and temperature. Species-specific Mg isotope offsets cannot be readily linked to calcification rate (Pogge von Strandmann, 2008) or habitat. As all foraminifera analysed to date are isotopically lighter than inorganic calcite, the data are best explained if Ca is pumped into an intracellular vacuole from seawater. We suggest that the efficiency of this pump determines the Mg isotope fractionation and speculate that

this pump selects light Mg isotopes preferentially. A recent model of Mg / Ca fractionation by a combination of transmembrane transport and passive transport (Nehrke et al., 2013) cannot explain the Mg isotope data, because the direction of isotope fractionation is wrong. This suggests that future models of Mg / Ca uptake into foraminifers should incorporate Ca and Mg isotope fractionation.

Single, calibrated foraminifera species may be used to reconstruct past seawater. Seawater δ^{26}Mg values inferred from the foraminiferal record are isotopically heavier than the present for most of the past 40 Ma, by up to ~ 0.8 ‰ , aside from isotopically light ratios during the late Oligocene. Dynamic box models of the various Mg sinks and sources to seawater suggest that the primary controls on seawater Mg concentrations and isotope ratios are the dolomite formation flux and the riverine flux, with the hydrothermal flux and riverine isotope ratios being more minor controls. Hence the low seawater δ^{26}Mg values observed at the present day and in the Oligocene appear to be due to relatively little dolomite formation, in both cases occurring at the same time as major climate cooling. Concomitant increases in δ^{7}Li and δ^{18}O together with decreasing δ^{26}Mg from ~ 15 Ma further suggest strong links between the cooling trend, changes in the weathering regime and significantly lower dolomite formation.

Author contributions. P. A. E. Pogge von Strandmann wrote the manuscript, designed the model and measured some of the samples. J. Forshaw picked and analysed most of the samples. D. N. Schmidt designed the project with P. A. E. Pogge von Strandmann, picked samples and edited the manuscript.

Acknowledgements. Derek Vance is thanked for discussions on the Mg budget of the oceans, and for reading a manuscript draft. Edward Tipper and John Higgins are thanked for extremely useful comments on an earlier version of the manuscript, and Frank Wombacher and an anonymous reviewer for comments on this version. P. A. E. Pogge von Strandmann is funded by NERC Research Fellowship NE/I020571/1 and DNS by a Royal Society URF.

Edited by: D. Gillikin

References

Anand, P., Elderfield, H., and Conte, M. H.: Calibration of Mg / Ca thermometry in planktonic foraminifera from a sediment trap time series, Paleoceanography, 18, doi:10.1029/2002PA000846, 2003.

Bentov, S. and Erez, J.: Impact of biomineralization processes on the Mg content of foraminiferal shells: A biological perspective, Geochem. Geophys. Geosyst., 7, doi:10.1029/2005gc001015, 2006.

Berner, E. K. and Berner, R. A.: Global Environment: Water, Air and Geochemical Cycles, Prentice Hall, 1996.

Berner, R. A.: GEOCARB II: A revised model of atmospheric CO_2 over Phanerozoic time, Am. J. Sci., 294, 56–91, 1994.

Berner, R. A., Lasaga, A. C., and Garrels, R. M.: The Carbonate-Silicate Geochemical Cycle and Its Effect on Atmospheric Carbon-Dioxide over the Past 100 Million Years, Am. J. Sci., 283, 641–683, 1983.

Black, J. R., Yin, Q. Z., and Casey, W. H.: An experimental study of magnesium-isotope fractionation in chlorophyll-a photosynthesis, Geochim. Cosmochim. Acta, 70, 4072–4079, 2006.

Bolou-Bi, E. B., Vigier, N., Poszwa, A., and Brenot, A.: Compared Mg isotope compositions of plants, rocks and waters, Geochim. Cosmochim. Acta, 71, A106, 2007.

Bolou-Bi, E. B., Vigier, N., Poszwa, A., Boudot, J.-P., and Dambrine, E.: Effects of biogeochemical processes on magnesium isotope variations in a forested catchment in the Vosges Mountains (France), Geochim. Cosmochim. Acta, 87, 341–355, 2012.

Busenberg, E. and Plummer, L. N.: Thermodynamics of magnesian calcite solid-solutions at 25 °C and 1 atm total pressure, Geochim. Cosmochim. Acta, 53, 1189-1208, doi:10.1016/0016-7037(89)90056-2, 1989.

Chang, V. T. C., Williams, R. J. P., Makishima, A., Belshawl, N. S., and O'Nions, R. K.: Mg and Ca isotope fractionation during CaCO3 biomineralisation, Biochem. Bioph. Res. Co., 323, 79–85, 2004.

Coggon, R. M., Teagle, D. A. H., Smith-Duque, C. E., Alt, J. C., and Cooper, M. J.: Reconstructing Past Seawater Mg / Ca and Sr / Ca from Mid-Ocean Ridge Flank Calcium Carbonate Veins, Science, 327, 1114–1117, doi:10.1126/science.1182252, 2010.

Coltice, N., Seton, M., Rolf, T., Mueller, R. D., and Tackley, P. J.: Convergence of tectonic reconstructions and mantle convection models for significant fluctuations in seafloor spreading, Earth Planet. Sci. Lett., 383, 92–100, doi:10.1016/j.epsl.2013.09.032, 2013.

Conrad, C. P. and Lithgow-Bertelloni, C.: Faster seafloor spreading and lithosphere production during the mid-Cenozoic, Geology, 35, 29–32, doi:10.1130/g22759a.1, 2007.

de Nooijer, L. J., Spero, H. J., Erez, J., Bijma, J., and Reichart, G. J.: Biomineralization in perforate Foraminifera, Earth-Sci. Rev., 135, 48–58, 2014.

de Villiers, S., Dickson, J. A. D., and Ellam, R. M.: The composition of the continental river weathering flux deduced from seawater Mg isotopes, Chem. Geol., 216, 133–142, 2005.

Elderfield, H. and Ganssen, G.: Past temperature and δ^{18}O of surface ocean waters inferred from foraminiferal Mg / Ca ratios, Nature, 405, 442–445, 2000.

Elderfield, H. and Schultz, A.: Mid-ocean ridge hydrothermal fluxes and the chemical composition of the ocean, Annu. Rev. Earth Pl. Sc., 24, 191-224, 1996.

Elderfield, H., Vautravers, M., and Cooper, M.: The relationship between shell size and Mg / Ca, Sr / Ca, δ^{18}, and δ^{13}C of species of planktonic foraminifera, Geochem. Geophys. Geosyst., 3, doi:10.1029/2001gc000194, 2002.

Elderfield, H., Yu, J., Anand, P., Kiefer, T., and Nyland, B.: Calibrations for benthic foraminiferal Mg / Ca paleothermometry and the carbonate ion hypothesis, Earth Planet. Sci. Lett., 250, 633–649, doi:10.1016/j.epsl.2006.07.041, 2006.

Erez, J.: The source of ions for biomineralization in foraminifera and their implications for paleoceanographic proxies, Rev. Mineral. Geochem., 54, 115–149, 2003.

Fantle, M. S. and DePaolo, D. J.: Sr isotopes and pore fluid chemistry in carbonate sediment of the Ontong Java Plateau: Calcite recrystallization rates and evidence for a rapid rise in seawater Mg over the last 10 million years, Geochim. Cosmochim. Acta, 70, 3883–3904, 2006.

Ferguson, J. E., Henderson, G. M., Kucera, M., and Rickaby, R. E. M.: Systematic change of foraminiferal Mg / Ca ratios across a strong salinity gradient, Earth Planet. Sci. Lett., 265, 153–166, doi:10.1016/j.epsl.2007.10.011, 2008.

Foster, G. L., Pogge von Strandmann, P. A. E., and Rae, J. W. B.: The boron and magnesium isotopic composition of seawater, Geochem. Geophys. Geosyst., 11, Q08015, doi:10.1029/2010GC003201, 2010.

Gaillardet, J., Dupre, B., Louvat, P., and Allegre, C. J.: Global silicate weathering and CO_2 consumption rates deduced from the chemistry of large rivers, Chem. Geol., 159, 3–30, 1999.

Galy, A., France-Lanord, C., and Derry, L. A.: The strontium isotopic budget of Himalayan Rivers in Nepal and Bangladesh, Geochim. Cosmochim. Acta, 63, 1905–1925, 1999.

Galy, A., Bar-Matthews, M., Halicz, L., and O'Nions, R. K.: Mg isotopic composition of carbonate: insight from speleothem formation, Earth Planet. Sci. Lett., 201, 105–115, 2002.

Georg, R. B., West, A. J., Vance, D., Newman, K., and Halliday, A. N.: Is the marine osmium isotope record a probe for CO_2 release from sedimentary rocks?, Earth Planet. Sci. Lett., 367, 28–38, 2013.

Geske, A., Zorlu, J., Richter, D. K., Buhl, D., Niedermayr, A., and Immenhauser, A.: Impact of diagenesis and low grade metamorphosis on isotope (δ^{26}Mg, δ^{13}C, δ^{18}O and 87Sr / 86Sr) and elemental (Ca, Mg, Mn, Fe and Sr) signatures of Triassic sabkha dolomites, Chem. Geol., 332–333, 45–64, 2012.

Hay, W. W.: The Pleistocene-Holocene fluxes are not the Earth's norm, in: Material fluxes on the surface of the Earth, National Academy Press, Washington D.C., 1994.

Higgins, J. A. and Schrag, D. P.: Constraining magnesium cycling in marine sediments using magnesium isotopes, Geochim. Cosmochim. Ac., 74, 5039–5053, 2010a.

Higgins, J. A. and Schrag, D. P.: Constraining magnesium cycling in marine sediments using magnesium isotopes, Geochim. Cosmochim. Ac., 74, 2039–5053, 2010b.

Higgins, J. A. and Schrag, D. P.: Records of Neogene seawater chemistry and diagenesis in deep-sea carbonate sediments and pore fluids, Earth Planet. Sci. Lett., 357–358, 386–396, 2012.

Hippler, D., Buhl, D., Witbaard, R., Richter, D. K., and Immenhauser, A.: Towards a better understanding of magnesium-isotope ratios from marine skeletal carbonates, Geochim. Cosmochim. Ac., 73, 6134–6146, doi:10.1016/j.gca.2009.07.031, 2009.

Holland, H. D.: Sea level, sediments and the composition of seawater, Am. J. Sci., 305, 220–239, 2005.

Holland, H. D. and Zimmermann, H.: The Dolomite Problem Revisited, Int. Geol. Rev., 42, 481–490, 2000.

Horita, J., Zimmermann, H., and Holland, H. D.: Chemical evolution of seawater during the Phanerozoic: Implications from the record of marine evaporites, Geochim. Cosmochim. Ac., 66, 3733–3756, 2002.

Huang, K. J., Teng, F. Z., Wei, G. J., Ma, J. L., and Bao, Z. Y.: Adsorption- and desorption-controlled magnesium isotope fractionation during extreme weathering of basalt in Hainan Island, China, Earth Planet. Sci. Lett., 359–360, 73–83, 2012.

Immenhauser, A., Buhl, D., Richter, D., Niedermayr, A., Riechelmann, D., Dietzel, M., and Schulte, U.: Magnesium-isotope fractionation during low-Mg calcite precipitation in a limestone cave – Field study and experiments, Geochim. Cosmochim. Ac., 74, 4346–4364, doi:10.1016/j.gca.2010.05.006, 2010.

John, C. M., Karner, G. D., Browning, E., Mark Leckie, R., and Mateo, Z.: Timing and magnitude of Miocene eustasy derived from the mixed siliciclastic-carbonate stratigraphic record of the northeastern Australian margin, Earth Planet. Sci. Lett., 304, 455–467, 2011.

Kisakürek, B., James, R. H., and Harris, N. B. W.: Li and δ^7Li in Himalayan rivers: Proxies for silicate weathering?, Earth Planet. Sci. Lett., 237, 387–401, 2005.

Kozdon, R., Kelly, D. C., Kitajima, K., Strickland, A., Fournelle, J. H., and Valley, J. W.: In situ δ^{18}O and Mg / Ca analyses of diagenetic and planktic foraminiferal calcite preserved in a deep-sea record of the Paleocene-Eocene thermal maximum, Paleoceanography, 28, 517–528, doi:10.1002/palo.20048, 2013.

Kump, L. R., Brantley, S. L., and Arthur, M. A.: Chemical, weathering, atmospheric CO_2, and climate, Ann. Rev. Earth Pl. Sc., 28, 611–667, 2000.

Lea, D. W., Mashiotta, T. A., and Spero, H. J.: Controls on magnesium and strontium uptake in planktonic foraminifera determined by live culturing, Geochim. Cosmochim. Ac., 63, 2369–2379, 1999.

Lear, C. H., Elderfield, H., and Wilson, P. A.: Cenozoic deep-sea temperatures and global ice volumes from Mg / Ca in benthic foraminiferal calcite, Science, 287, 269–272, doi:10.1126/science.287.5451.269, 2000.

Lear, C. H., Elderfield, H., and Wilson, P. A.: A Cenozoic seawater Sr / Ca record from benthic foraminiferal calcite and its application in determining global weathering fuxes, Earth Planet. Sci. Lett., 208, 69–84, 2003.

Levasseur, S., Birck, J. L., and Allègre, C. J.: The osmium riverine flux and the oceanic mass balance of osmium, Earth Planet. Sci. Lett., 174, 7–23, 1999.

Li, G. and West, A. J.: Evolution of Cenozoic seawater lithium isotopes: Coupling of global denudation regime and shifting seawater sinks, Earth Planet. Sci. Lett., 401, 284–293, 2014.

Li, G., Ji, J., Chen, J., and Kemp, D. B.: Evolution of the Cenozoic carbon cycle: The roles of tectonics and CO_2 fertilization, Global Biogeochem. Cy., 23, GB1009, doi:10.1029/2008GB003220, 2009a.

Li, G., Ji, J., and Kemp, D. B.: Evolution of the Cenozoic carbon cycle: The roles of tectonics and CO_2 fertilization, Global Biogeochem. Cy., 23, GB1009, doi:10.1029/2008GB003220, 2009b.

Li, W. Q., Chakraborty, S., Beard, B. L., Romanek, C. S., and Johnson, C. M.: Magnesium isotope fractionation during precipitation of inorganic calcite under laboratory conditions, Earth Planet. Sci. Lett., 333, 304–316, doi:10.1016/j.epsl.2012.04.010, 2012.

Li, W.-Y., Teng, F. Z., Ke, S., Rudnick, R. L., Gao, S., Wu, F.-Y., and Chappell, B. W.: Heterogeneous magnesium isotopic composition of the upper continental crust, Geochim. Cosmochim. Ac., 74, 6867–6884, 2010.

Martinez-Boti, M. A., Mortyn, P. G., Schmidt, D. N., Vance, D., and Field, D. B.: Mg / Ca in foraminifera from plankton tows: Evaluation of proxy controls and comparison with core tops, Earth Planet. Sci. Lett., 307, 113–125, doi:10.1016/j.epsl.2011.04.019, 2011.

McArthur, J. M., Howarth, R. J., and Bailey, T. R.: Strontium isotope stratigraphy: LOWESS version 3: Best fit to the marine Sr-isotope curve for 0-509 Ma and accompanying look-up table for deriving numerical age, J. Geol., 109, 155–170, 2001.

Millot, R., Vigier, N., and Gaillardet, J.: Behaviour of lithium and its isotopes during weathering in the Mackenzie Basin, Canada, Geochim. Cosmochim. Ac., 74, 3897–3912, 2010.

Misra, S. and Froelich, P. N.: Lithium Isotope History of Cenozoic Seawater: Changes in Silicate Weathering and Reverse Weathering, Science, 335, 818–823, 2012.

Mottl, M. J. and Wheat, C. G.: Hydrothermal circulation through mid-ocean ridge flanks: Fluxes of heat and magnesium, Geochim. Cosmochim. Ac., 58, 2225–2237, 1994.

Mucci, A.: Influence of temperature on the composition of magnesian calcite overgrowths precipitated from seawater, Geochim. Cosmochim. Ac., 51, 1977–1984, doi:10.1016/0016-7037(87)90186-4, 1987.

Muller, R. D., Sdrolias, M., Gaina, C., Steinberger, B., and Heine, C.: Long-term sea-level fluctuations driven by ocean basin dynamics, Science, 319, 1357–1362, doi:10.1126/science.1151540, 2008.

Nehrke, G., Keul, N., Langer, G., de Nooijer, L. J., Bijma, J., and Meibom, A.: A new model for biomineralization and trace-element signatures of Foraminifera tests, Biogeosciences, 10, 6759–6767, doi:10.5194/bg-10-6759-2013, 2013.

Ni, Y., Foster, G. L., Bailey, T., Elliott, T., Schmidt, D. N., Pearson, P. N., Haley, B., and Coath, C. D.: A core top assessment of proxies for the ocean carbonate system in surface-dwelling foraminifers, Paleoceanography, 22, PA3212, 2007.

Nürnberg, D., Bijma, J., and Hemleben, C.: Assessing the reliability of magnesium in foraminiferal calcite as a proxy for water mass temperatures, Geochim. Cosmochim. Ac., 60, 2483–2483, 1996.

Oliver, L., Harris, N., Bickle, M., Chapman, H., Dise, N., and Horstwood, M.: Silicate weathering rates decoupled from the $^{87}Sr/^{86}Sr$ ratio of the dissolved load during Himalayan erosion, Chem. Geol., 201, 119–139, 2003.

Opdyke, B. N. and Wilkinson, B. H.: Surface area control of shallow cratonic to deep marine carbonate accumulation, Paleoceanography, 3, 685–703, 1988.

Palmer, M. R. and Edmond, J. M.: Controls over the strontium isotope composition of river water, Geochim. Cosmochim. Ac., 56, 2099–2111, 1992.

Pogge von Strandmann, P. A. E.: Precise magnesium isotope measurements in core top planktic and benthic foraminifera, Geochem. Geophys. Geosyst., 9, Q12015, doi:10.1029/2008GC002209, 2008.

Pogge von Strandmann, P. A. E., Burton, K. W., James, R. H., van Calsteren, P., and Gislason, S. R.: The influence of weathering processes on riverine magnesium isotopes in a basaltic terrain, Earth Planet. Sci. Lett., 276, 187–197, 2008.

Pogge von Strandmann, P. A. E., Elliott, T., Marschall, H. R., Coath, C., Lai, Y. J., Jeffcoate, A. B., and Ionov, D. A.: Variations of Li and Mg isotope ratios in bulk chondrites and mantle xenoliths, Geochim. Cosmochim. Ac., 75, 5247–5268, 2011.

Pogge von Strandmann, P. A. E., Opfergelt, S., Lai, Y. J., Sigfusson, B., Gislason, S. R., and Burton, K. W.: Lithium, magnesium and silicon isotope behaviour accompanying weathering in a basaltic soil and pore water profile in Iceland, Earth Planet. Sci. Lett., 339–340, 11–23, 2012.

Ra, K., Kitagawa, H., and Shiraiwa, Y.: Mg isotopes in chlorophyll-a and coccoliths of cultured coccolithophores (Emiliania huxleyi) by MC-ICP-MS, Mar. Chem., 122, 130–137, 2010.

Raitzsch, M., Dueñas-Bohórquez, A., Reichart, G.-J., de Nooijer, L. J., and Bickert, T.: Incorporation of Mg and Sr in calcite of cultured benthic foraminifera: impact of calcium concentration and associated calcite saturation state, Biogeosciences, 7, 869–881, doi:10.5194/bg-7-869-2010, 2010.

Richter, F. M., Mendybaev, R. A., Christensen, J. N., Hutcheon, I. D., Williams, R. W., Sturchio, N. C., and Belsos Jr., A. D.: Kinetic isotopic fractionation during diffusion of ionic species in water, Geochim. Cosmochim. Ac., 70, 277–289, 2006.

Saenger, C. and Wang, Z.: Magnesium isotope fractionation in biogenic and abiogenic carbonates: implications for paleoenvironmental proxies, Quaternary Sci. Rev., 90, 1–21, 2014.

Saulnier, S., Rollion-Bard, C., Vigier, N., and Chaussidon, M.: Mg isotope fractionation during calcite precipitation: An experimental study, Geochim. Cosmochim. Ac., 91, 75–91, doi:10.1016/j.gca.2012.05.024, 2012.

Shackleton, N. J. and Kennett, J. P.: Paleotemperature history of the Cenozoic and the initiation of Antarctic glaciation: oxygen and carbon isotope analysis is DSDP Sites 277, 279, and 281, in: Initial Reports of the Deep Sea Drilling Project, US Government Printing Office, 1975.

Teng, F. Z., Li, W. Y., Ke, S., Marty, B., Dauphas, N., Huang, S., Wu, F.-Y., and Pourmand, A.: Magnesium isotopic composition of the Earth and chondrites, Geochim. Cosmochim. Ac., 74, 4150–4166, 2010a.

Teng, F. Z., Li, W. Y., Rudnick, R. L., and Gardner, L. R.: Contrasting lithium and magnesium isotope fractionation during continental weathering, Earth Planet. Sci. Lett., 300, 63–71, 2010b.

ter Kuile, B.: Mechanisms for calcification and carbon cycling in algal symbiont-bearing foraminifera, in: Biology of Foraminifera, edited by: Lee, J. J. and Anderson, O. R., Academic Press Limited, 73–92, 1991.

Tipper, E. T., Galy, A., and Bickle, M. J.: Riverine evidence for a fractionated reservoir of Ca and Mg on the continents: Implications for the oceanic Ca cycle, Earth Planet. Sci. Lett., 247, 267–279, 2006a.

Tipper, E. T., Galy, A., Gaillardet, J., Bickle, M. J., Elderfield, H., and Carder, E. A.: The magnesium isotope budget of the modern ocean: Constraints from riverine magnesium isotope ratios, Earth Planet. Sci. Lett., 250, 241–253, 2006b.

Tipper, E. T., Galy, A., and Bickle, M.: Calcium and magnesium isotope systematics in rivers draining the Himalaya-Tibetan-Plateau region: Lithological or fractionation control?, Geochim. Cosmochim. Ac., 72, 1057–1075, 2008.

Tipper, E. T., Gaillardet, J., Louvat, P., Capmas, F., and White, A. F.: Mg isotope constraints on soil pore-fluid chemistry: Evidence from Santa Cruz, California, Geochim. Cosmochim. Ac., 74, 3883–3896, 2010.

Tipper, E. T., Calmels, D., Gaillardet, J., Louvat, P., Capmas, F., and Dubacq, B.: Positive correlation between Li and Mg isotope ratios in the river waters of the Mackenzie Basin

challenges the interpretation of apparent isotopic fractionation during weathering, Earth Planet. Sci. Lett., 333, 35–45, doi:10.1016/j.epsl.2012.04.023, 2012.

Vance, D., Teagle, D. A. H., and Foster, G. L.: Variable Quaternary chemical weathering fluxes and imbalances in marine geochemical budgets, Nature, 458, 493–496, 2009.

Walker, J. C. G., Hays, P. B., and Kasting, J. F.: A Negative Feedback Mechanism for the Long-Term Stabilization of Earths Surface-Temperature, J. Geophys. Res.-Oc. Atm., 86, 9776–9782, 1981.

Wanner, C., Sonnenthal, E. L., and Liu, X.-M.: Seawater δ^7Li: A direct proxy for global CO_2 consumption by continental silicate weathering?, Chem. Geol., 381, 154–167, 2014.

Wimpenny, J., Burton, K. W., James, R. H., Gannoun, A., Mokadem, F., and Gislason, S. R.: The behaviour of magnesium and its isotopes during glacial weathering in an ancient shield terrain in West Greenland, Earth Planet. Sci. Lett., 304, 260–269, doi:10.1016/j.epsl.2011.02.008, 2011.

Wombacher, F., Eisenhauer, A., Bohm, F., Gussone, N., Regenberg, M., Dullo, W. C., and Ruggeberg, A.: Magnesium stable isotope fractionation in marine biogenic calcite and aragonite, Geochim. Cosmochim. Ac., 75, 5797–5818, doi:10.1016/j.gca.2011.07.017, 2011.

Yoshimura, T., Taniguchi, M., Inoue, M., Suzuki, A., Iwasaki, N., and Kawahata, H.: Mg isotope fractionation in biogenic carbonates of deep-sea coral, benthic foraminifera, and hermatypic coral, Anal. Bioanal. Chem., 401, 2755–2769, 2011.

Young, E. D. and Galy, A.: The isotope geochemistry and cosmochemistry of magnesium, in: Geochemistry of non-traditional stable isotopes, edited by: Johnson, C. M., Beard, B. L., and Albarede, F., Mineralogical Society of America, Geochemical Society, Washington D.C., 197–230, 2004.

Zachos, J. C., Pagani, M., Sloan, L., Thomas, E., and Billups, K.: Trends, rhythms, and aberrations in global climate 65 Ma to present, Science, 292, 686–693, 2001.

Zachos, J. C., Kroon, D., Blum, P., Bowles, J., Gaillot, P., Hasegawa, T., Hathorne, E. C., Hodell, D. A., Kelly, D. C., Jung, J.-H., Keller, S. M., Lee, Y. S., Leuschner, D. C., Liu, Z., Lohmann, K. C., Lourens, L., Monechi, S., Nicolo, M., Raffi, I., Riesselman, C., Röhl, U., Schellenberg, S. A., Schmidt, D., Sluijs, A., Thomas, D., Thomas, E., and Vallius, H.: Proceedings of the Ocean Drilling Program, Initial Reports Volume 208, College Station TX (Ocean Drilling Program), 1–112, 2004.

Zimmermann, H.: Tertiary seawater chemistry – Implications from primary fluid inclusions in marine halite, Am. J. Sci., 300, 723–767, 2000.